Analytic method for observation of the gravity waves using radio occultation data

Y. A. Liou,[1,2] A. G. Pavelyev,[1,3] C. Y. Huang,[2] K. Igarashi,[4] K. Hocke,[4] and S. K. Yan[1]

Received 25 May 2003; revised 21 August 2003; accepted 15 September 2003; published 16 October 2003.

[1] We present an analytical method for observation of the gravity waves (GWs) in the atmosphere from the amplitude of the radio occultation (RO) signal. We found the height dependence of the GW phase and amplitude (the GW "*portrait*") using for example the amplitude data corresponding to one of the GPS/Meteorology (GPS/MET) RO events. We estimated the horizontal wind speed perturbations, which are in fairly good agreement with radiosonde data. The horizontal wind speed perturbations v(h) are changing in the range v ∼ ± 1–±9 m/s with vertical gradients dv/dh ∼ ± 0.5–±15 m/(s km) in the height interval 10–40 km. The height dependence of the GW vertical wavelength has been inferred through the differentiation of the GW phase. Analysis of this dependence gives the estimation of the GW intrinsic phase speed, which varies for the considered event in the interval 1.5–5 m/s. Thus the analytical method has the capability to extract important information from the amplitude of the RO signals helpful for studying the GW activity in the atmosphere. *INDEX TERMS:* 0350 Atmospheric Composition and Structure: Pressure, density, and temperature; 3384 Meteorology and Atmospheric Dynamics: Waves and tides; 6964 Radio Science: Radio wave propagation; 6969 Radio Science: Remote sensing; 6904 Radio Science: Atmospheric propagation. **Citation:** Liou, Y. A., A. G. Pavelyev, C. Y. Huang, K. Igarashi, K. Hocke, and S. K. Yan, Analytic method for observation of the gravity waves using radio occultation data, *Geophys. Res. Lett.*, *30*(20), 2021, doi:10.1029/2003GL017818, 2003.

1. Introduction

[2] GWs play a decisive role in affecting the atmospheric circulation and temperature regime [*Friits and Alexander*, 2003]. For theoretical studies of the GWs phenomena it is important to have the experimental data showing the phase and amplitude dependence of the GWs on height. Radiosonde and rocketsonde GWs measurements, balloon soundings, radar observations, and lidar studies have been limited to the ground-based sites [*Eckermann et al.*, 1995; *Steiner et al.*,1999] mainly over specific land parts of the Northern Hemisphere. Nowadays the RO method can be applied to measure the GW parameters in the global scale. The radio signals emitted at two GPS frequencies F1 = 1575.42 and F2 = 1227.6 MHz by the radio navigational satellites and received by a small satellite installed on a low earth orbit (LEO) have been used for the RO investigations [*Kursinski et al.*, 1997; *Steiner et al.*, 1999].

[3] Analysis of the temperature variations found from the RO phase data furnishes an opportunity to investigate the global morphology of the GWs activity in the stratosphere and to measure the GWs statistical characteristics in the atmosphere as shown by *Tsuda et al.* [2000], *Steiner and Kirchengast* [2000], and *Tsuda and Hocke* [2002]. However these papers concerned mainly with the GW statistical parameters. The amplitude channels of the RO signal give new potential and capability for the RO research and for the observation of the quasi-regular structures in the atmospheric and ionospheric waves [*Kalashnikov et al.*, 1986; *Pavelyev et al.*, 2002a, 2002b; *Sokolovskiy*, 2000; *Igarashi et al.*, 2000, 2001; *Liou et al.*, 2002]. The aim of this paper is to demonstrate the possibility of direct observation of the quasi-regular internal waves in the atmosphere using the amplitude of the RO signals.

2. Wave Trains in the RO Data

[4] The scheme of the RO experiment is shown in Figure 1. The point O is the center of the spherical symmetry of the atmosphere. Radio waves emitted by the GPS satellite (point G) are propagating to the receiver (point L) along the ray GTL. T is the tangent point in the atmosphere where the ray's height h is minimal. The projection of the point T on the Earth surface point D determines the coordinates of the RO region: latitude φ and longitude λ_l. The longitude λ_l is reckoned between the Greenwich M_g and the RO meridian M_o (Figure 1). Record of the RO signal along the LEO trajectory contains the amplitudes A1(t), A2(t) and phases of the radio field at frequencies F1, F2 as functions of time. The time interval for RO measurements τ depends on the orientation between the vertical direction at the point T and the occultation beam path. The time τ is minimal ∼30 s, when the orbital planes of the LEO and GPS satellites are parallel. Thus RO experiments record practically simultaneously the impact of the GWs on the RO signal because the GW frequencies are usually well below $1/\tau \sim 0.03\ s^{-1}$. The horizontal resolution of the RO amplitude method 2L is equal to the length of coherent interaction L_c between the RO signal and the atmosphere [*Igarashi et al.*, 2001]. In the case of spherical symmetry the main contribution to the amplitude of the RO signal introduced relatively small area along the ray GTL with center at the tangent point T (Figure 1). In this area the direction angle α of the ray trajectory relative to the local vertical is near zero. We can estimate the length of this

[1]Center for Space and Remote Sensing Research, National Central University, Chung-Li, Taiwan.
[2]Institute of Space Science, National Central University, Chung-Li, Taiwan.
[3]Institute of Radio Engineering and Electronics of Russian Academy of Sciences, (IRE RAS), Moscow region, Russia.
[4]Communication Research Laboratory, Independent Administrative Institute, Tokyo, Japan.

0094-8276/03/2003GL017818$05.00

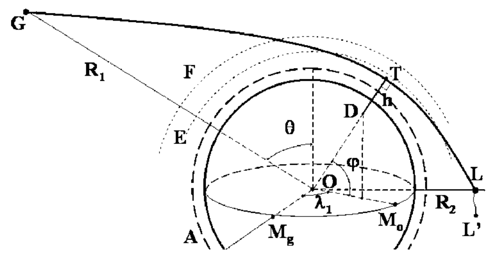

Figure 1. Key physical and geometric parameters of the RO measurements.

area L_c and the value α at its boundary using simple consideration. The angle α is connected with $L = L_c/2$: $\alpha = L/a$ (A), where a is the distance OT. For coherent interaction the angle α does not exceed the Fresnel's zone angular size $\alpha \leq [\lambda X/(2L)]^{1/2}$ (B), where X is the refraction attenuation of the radio wave at T. From comparison of the formulas (A), (B) one obtains $\alpha \leq (\lambda X/a)^{1/3}$ (C). It follows from (A), (C) that the length of coherent interaction L_c and vertical resolution Δh are equal to $2^{2/3}a^{2/3}\lambda^{1/3}X^{1/3}$ and $2^{-2/3}a^{1/3}\lambda^{2/3}\ X^{2/3}$, respectively. For $X = 1$, $\lambda = 20$ cm, $a = 6400$ km, $\Delta h \approx 40$ m, and $L_c = 2L \approx 32$ km. Thus the RO amplitude method is sensitive to the GW with vertical and horizontal wavelengths greater than 40 m and 32 km, respectively. The amplitudes of the RO signal (curves A1, A2) are shown in Figure 2a for the GPS/MET RO event 0316. Results of the simulations of the amplitude dependence on height are shown by the curves M0 and M. For calculations of the curves M0, M we use the radio physical model describing the refractivity profiles in the atmosphere [*Pavelyev et al.*, 1996; *Pavelyev*, 1998] and exact expression for the refraction attenuation [*Pavelyev and Kucherjavenkov*, 1978]. To obtain the vertical profiles of temperature and its gradient we use the expressions given by *Hocke* [1997], and *Pavelyev et al.* [2002b]. The wave trains with intense amplitude variations can be noted in the height interval 8–40 km. They have internal vertical wavelength changing in the range 0.8–2 km. The results of the simulation (the curves M0, M in Figure 2a) show a good fit to the experimental data, which corresponds to a reduced level of the systematic errors in the amplitude data and a sufficient accuracy of the model used for simulation. The amplitude changes correspond to the variations in the refractivity and temperature vertical gradients, which can be restored by the amplitude method described by *Kalashnikov et al.* [1986], and validated by *Pavelyev et al.* [2002a, 2002b], and *Liou et al.* [2002]. Vertical gradients of the temperature retrieved from the amplitude data are indicated in Figure 2b. Quasi–regular wave structure with vertical wavelength $\lambda_h \sim 0.8$–2 km is clearly seen both in the experimental and model data. We will use for succeeding analysis of GW the dispersion and polarization relationships, which are valid for the medium-frequency case, when the intrinsic frequency of the GWs is many times over the inertial frequency f, but is well below the buoyancy frequency ω_b. The vertical wavelength λ_h is connected with back-ground wind speed U by dispersion relation [*Eckerman et al.*, 1995; *Friits and Alexander*, 2003]

$$\lambda_h = 2\pi|c - U\cos\varphi|/\omega_b, \tag{1}$$

where c is the ground-based GWs horizontal phase speed, and φ is the azimuth angle between the background wind and the GW propagation vectors. Equation (1) connects λ_h with the intrinsic phase speed $v_i = |c - U\cos\varphi|$, which can

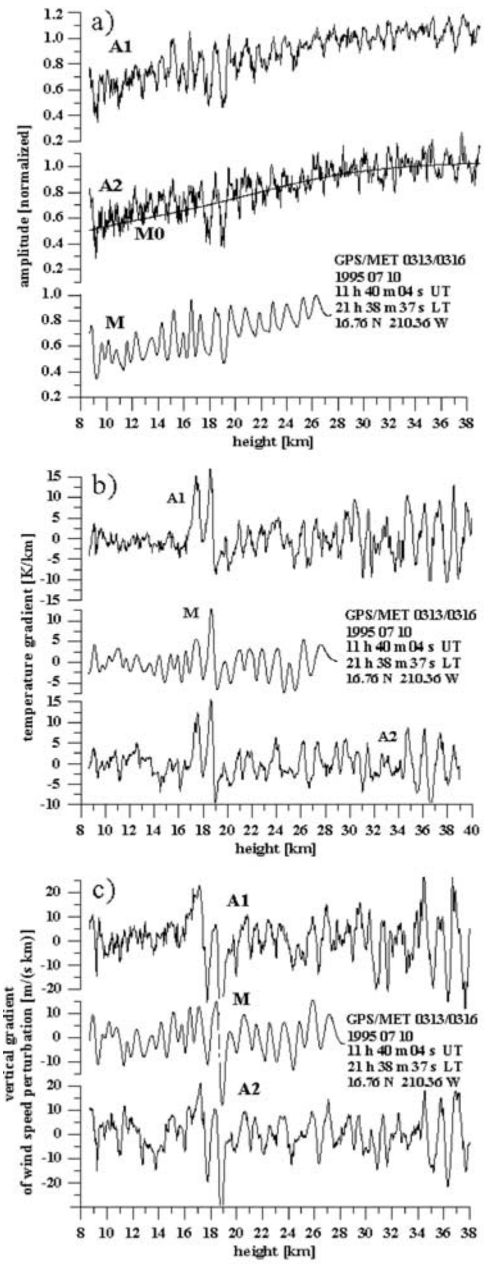

Figure 2. Panel (a) Wave train in the amplitudes A1, A2. Curves M0, M correspond to results of the amplitude evaluation using the standard (damped exponential) and wave (the sum of damped complex exponentials) models of the refractivity: $N(h) = \mathrm{Re}[N_o\exp(-\alpha h)]$ with real and complex α [*Pavelyev et al.*, 1996; *Pavelyev*, 1998]. Panel (b) Vertical gradient dt/dh retrieved from the amplitude RO data. Panel (c) Vertical gradient dv/dh restored from dt/dh. Curves A1, A2 correspond to the amplitudes A1, A2 in the RO signal, respectively. Curve M describes the simulation's results.

be measured by an observer moving with the back-ground wind velocity [*Eckerman et al.*, 1995]. The polarization relation, which is valid for intermediate frequency range, non-rotating case with back-ground flow depending only on height [*Lindzen*, 1993], connects the complex amplitude of the temperature variations, t(h), with the horizontal wind speed variations v(h), corresponding to the GW influence

$$v(h) = \mathrm{Re}[ig/(T_b\omega_b)t(h)], \omega_b^2 = g/T_b\Gamma, \Gamma = \partial T_b/\partial h + 9.8°/\mathrm{km}, \tag{2}$$

where g is the gravity acceleration, Γ is the adiabatic lapse rate, and T_b is the background temperature. *Pfister et al.* [1993] applied successfully this relation to the case study of the regular GWs associated with tropical cyclone. *Eckerman et al.* [1995] used it for statistical analysis of the rocketsonde data. *Tsuda et al.* [2000] applied relation (2) to determine a global distribution of the GW potential energy using the RO data. One obtains by differentiating (2)

$$dv(h)/dh = d\mathrm{Re}[(ig/T_b\omega_b)t(h)]/dh \approx \mathrm{Re}[ig/(T_b\omega_b)dt(h)/dh]. \tag{3}$$

Equation (3) is valid assuming that $T_b(h)$ and $\omega_b(h)$ are slowly changing at the vertical scales $\sim\lambda_h$. The functions T_b and ω_b are known from the model of the atmosphere used for the calculation of the refraction attenuation and refractivity in the RO region. To find the function dv(h)/dh from the second equation (3) one can implement the Hilbert transform, which evaluates the analytic presentation of the real signal dt(h)/dh:

$$dt(h)/dh = \mathrm{Re}\{a_t(h)\exp[i\Phi_t(h)]\}, \tag{4}$$

where $a_t(h)$ and $\Phi_t(h)$ are the amplitude and phase of the vertical gradient of the temperature. The function dv(h)/dh can be restored from (3) using the Hilbert transform. The results of restoration are indicated in Figure 2c. The quasi-regular modulation of dv/dh is clearly seen both in the experimental and model data. It is important that the vertical period of this modulation is practically the same as seen in the amplitude variations in Figure 2a. Thus the process of inversion of the amplitude data does not essentially change the form of the initial spectrum of the amplitude variations. One can directly obtain, without inversion, the approximations of the phase and amplitude parts of the function dv(h)/dh using the Hilbert transform of the variations in the amplitude of the RO signals normalized to the standard altitude dependence of the amplitude (shown by curve M0 in Figure 2). However the amplitude part of dv(h)/dh will be described in this case only by a qualitative manner because of the absence of important scaling factor, depending on height.

3. "Portrait" of Gravity Wave

[5] After applying the Hilbert transform one can obtain from (3), (4) the amplitude and phase a(h), Φ(h) associated with the vertical gradient of the horizontal wind speed

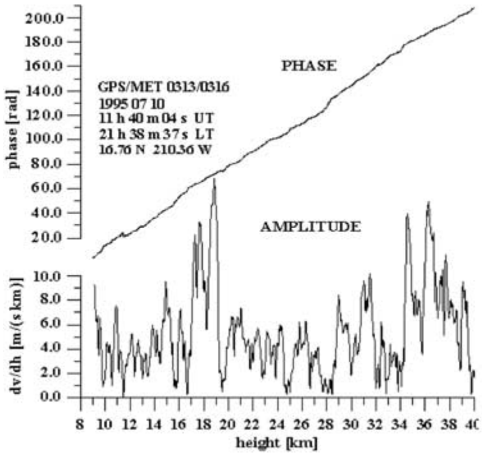

Figure 3. GW amplitude and phase as functions of height.

variations: $dv(h)/dh = [dv_{A1}(h)/dh + dv_{A2}(h)/dh]/2 = a(h) \cos \Phi(h)$, where a(h) and Φ(h) are the amplitude and phase of the analytic signal relevant to dv(h)/dh. Note, that summation of data of two independent amplitude channels A1, A2 can diminish the statistical and independent systematic errors in the experimental data The functions a(h), Φ(h) present together a GW *portrait*. The height dependence of the GW amplitude a(h) and phase Φ(h) are shown in Figure 3.

[6] The phase curve of the GW *portrait* depends linearly, in average, on the height h (Figure 3). The amplitude changes in the interval 0.5...16 m/(s km). One can note using the GW *portrait* (Figure 3) the altitudes with high (17–19 km, 29–31 km, 35–38 km) and low (32–34 km) GW activity. By differentiating the phase Φ(h) one can obtain the spatial frequency f_h and the vertical wavelength $\lambda_h = 1/f_h$ as functions of height and then estimate using the relation (1) the intrinsic phase speed of GW v_i (Figure 4a). As is seen in Figure 4a the value $v_i(h)$ changes in the range 1.5–5 m/s. This estimation may correspond to the quiet conditions in the atmosphere. Integration of the average wind speed gradients $dv/dh = [dv_{A1}(h)/dh + dv_{A2}(h)/dh]/2$ (Figure 2c) on height gives the horizontal wind perturbations v(h) associated with the GW influence. The function v(h) is depicted in Figure 4b. The curve A corresponds to the experimental data; the curve M describes the simulation results; and the curves 1–4 indicate the radiosondes (RS) data relating to two stations in Taiwan: Hualien (1,4) (24.0°N, 238.4°W) and Taipei (2,3) (25.0°N, 238.5°W) obtained on July 15, 1995 at 00 h UT (1,2) and 12 h UT (3,4), respectively. The difference between the Taiwan stations and the RO region latitudes and longitudes is $\sim$8° and $\sim$28°, respectively. The time difference between the RO and RS observations has been chosen in accordance with the average RS background westward wind velocity $\sim$10 m/s in the height interval 8–30 km. The RS wind perturbations (curves 1–4) have been obtained by subtracting the polynomial approximation of the fifth power from the experimental vertical profiles of the horizontal wind speed. As follows from Figure 4b the RS data (1–4) are in fairly good agreement with the experimental results (A). Some discrepancy $\sim$2–4 m/s exists in the height interval 20–30 km. The

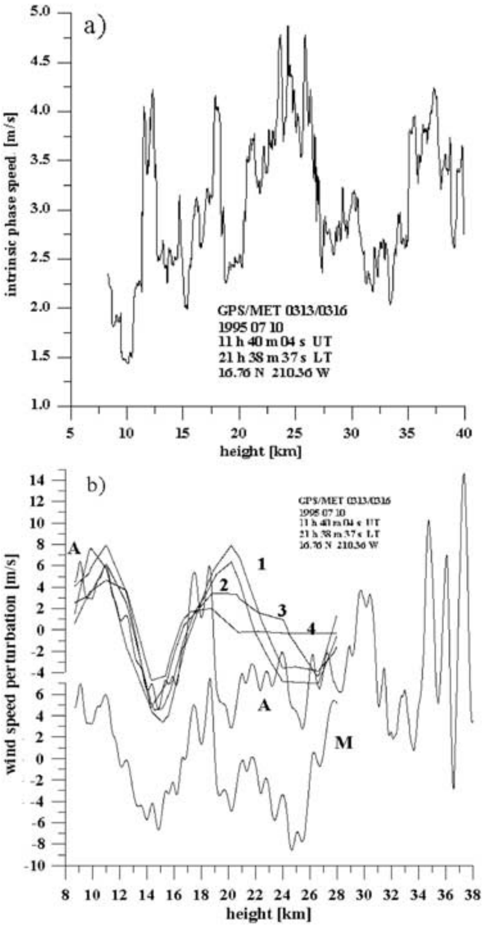

Figure 4. Panel (a) The GW intrinsic phase speed $v_i(h)$. Panel (b) Horizontal wind speed perturbations v(h) associated with GW influence. The curves indicate the v(h) profiles retrieved from the radiosondes data 1–4, amplitude data A, and model simulation M, respectively.

difference may correspond to a current state of the inversion accuracy. Note that RS data do not reveal high-spatial frequencies observed in the RO results. As appears this is due to smoothing effects of the RS measurements. Note also that difference between the RS and experimental data may be connected with the instability of the receiver gain and the transmitter power, and increasing low-frequency noise (which contains trends and bias) owing to integration during the inversion process. The RO values of v(h) (curve A) are variable from ±1–±9 m/s at the height interval 10–35 km and are in agreement with simulation results (curve M). This demonstrates the effectivness of the model used for simulation.

4. Conclusions

[7] The introduced analytic method demonstrates its capability to retrieve the GW *portrait* using the amplitude data of the RO signals. The GW *portrait* is restored using Hilbert transform in the form of the analytic signal containing the amplitude and phase of the GW as functions of height. The analytic form of the GW presentation is convenient for the analysis of the experimental data and can be implemented for the determination of the GW intrinsic phase speed and the horizontal wind speed perturbations associated with the GW influence. The radiosonde wind measurements rhymed satisfactorily with the wind speed perturbations retrieved from the RO data. The discrepancy is about 1–2 m/s for the heights below 18 km and ~2–4 m/s for the heights 20–30 km. Thus the RO method appears to have a promise to measure in global scale the regular characteristics of the GW.

[8] **Acknowledgments.** We are grateful to UCAR for access to the GPS/MET data, and to National Science Council of Taiwan, R.O.C., for financial support under the grants NSC 92-2811-M008-001, NSC 91-2111-M008-029, and Office of Naval Research (ONR) of USA under grant N00014-00-0528. Work is supported by Russian Fund of Basic Research, grant No. 03-02-17414.

References

Eckermann, S. D., I. Hirota, and W. A. Hocking, Gravity wave and equatorial wave morphology of the stratosphere derived from long-term rocket soundings, *Q. J. R. Meteorol. Soc.*, *121*, 149–186, 1995.

Friits, D. C., and M. J. Alexander, Gravity wave dynamics and effects in the middle atmosphere, *Rev. Geophys.*, *41*, 3-1–3-64, 2003.

Hocke, K., Inversion of GPS meteorology data, *Annales Geophysicae*, *15*, 443–450, 1997.

Igarashi, K., A. Pavelyev, K. Hocke, D. Pavelyev, and J. Wickert, Observation of wave structures in the upper atmosphere by radio holographic analysis of the RO data, *Adv. Space Res.*, *27*(6–7), 1321–1327, 2001.

Igarashi, K., A. Pavelyev, K. Hocke, D. Pavelyev, I. A. Kucherjavenkov, S. Matugov, A. Zakharov, and O. Yakovlev, Radio holographic principle for observing natural processes in the atmosphere and retrieving meteorological parameters from RO data, *Earth Planets Space*, *52*, 868–875, 2000.

Kalashnikov, I., S. Matugov, A. Pavelyev, and O. Yakovlev, Analysis of the RO method for the Earth's atmosphere study, In the book *Electromagnetic waves in the atmosphere and space*, 208–218. "Nauka" Ed. Moscow, (in Russian), 1986.

Kursinski, E. R., G. A. Hajj, J. T. Schofield, R. P. Linfield, and K. R. Hardy, Observing Earth's atmosphere with radio occultation measurements using the Global Positioning System, *J. Geophys. Res.*, *102*, 23,429–23,465, 1997.

Lindzen, R. S., Dynamics in Atmospheric Physics, chapter 10, Internal gravity waves, *2*, 204–217, Cambridge Univ. Press, 1993.

Liou, Y.-A., A. G. Pavelyev, C.-Y. Huang, K. Igarashi, and K. Hocke, Simultaneous observation of the vertical gradients of refractivity in the atmosphere and electron density in the lower ionosphere by radio occultation amplitude method, *Geophys. Res. Lett.*, *29*(19), 43-1–43-4, 2002.

Pavelyev, A., K. Igarashi, C. Reigber, K. Hocke, J. Wickert, G. Beyerle, S. Matyugov, A. Kucherjavenkov, D. Pavelyev, and O.I. Yakovlev, First application of the radio holographic method to wave observations in the upper atmosphere, *Radio Sci.*, *37*(3), pp. 15-1–15-11, 2002a.

Pavelyev, A. G., and A. I. Kucherjavenkov, Refraction attenuation in the planetary atmospheres, *Radio Eng. and Electron. Phys.*, *23*(7), 13–19, 1978.

Pavelyev, A. G., Y. A. Liou, C. Y. Huang, C. Reigber, J. Wickert, K. Igarashi, and K. Hocke, Radio holographic method for the study of the ionosphere, atmosphere and terrestrial surface from space using GPS occultation signals, *GPS Solutions*, *6*, 101–108, 2002b.

Pavelyev, A., A. V. Volkov, A. I. Zakharov, S. A. Krytikh, and A. I. Kucherjavenkov, Bistatic radar as a tool for earth investigation, *Acta Astronautica*, *39*, 721–730, 1996.

Pavelyev, A., On the possibility of radio holographic investigation on communication link satellite-to-satellite, *J. Communications Technology and Electronics*, *43*(8), 126–131, 1998.

Pfister, L., K. R. Chan, T. P. Bui, S. Bowen, M. Legg, B. Gary, K. Kelly, M. Proffit, and W. Starr, Gravity waves generated by a tropical cyclone during the STEP tropical field program: A case study, *J. Geophys. Res.*, *98*(D5), 8611–8638, 1993.

Sokolovskiy, S. V., Inversion of radio occultation amplitude data, *Radio Sci.*, *35*(1), 97–105, 2000.

Steiner, A. K., and G. Kirchengast, Gravity wave spectra from GPS/MET occultation observations, *J. Atmos. Ocean. Tech.*, *17*, 495–503, 2000.

Steiner, A. K., G. Kirchengast, and H. P. Landreiter, Inversion, error analysis, and validation of GPS/MET occultation data, *Ann. Geophys.*, *17*, 122–138, 1999.

Tsuda, T., and K. Hocke, Vertical wave number spectrum of temperature fluctuations in the stratosphere using GPS occultation data, *J. Meteorol. Soc. Japan*, *80*(4B), 1–13, 2002.

Tsuda, T., M. Nishida, C. Rocken, and R. H. Ware, A global morphology of gravity wave activity in the stratosphere revealed by the GPS occultation data (GPS/MET), *J. Geophys. Res.*, *105*, 7257–7273, 2000.

Y. A. Liou and S. K. Yan, Center for Space and Remote Sensing Research, National Central University, Chung-Li, 320, Taiwan. (yueian@csrsr.ncu.edu.tw)

C. Y. Huang, Institute of Space Science, National Central University, Chung-Li, 320, Taiwan.

A. G. Pavelyev, Institute of Radio Engineering and Electronics of Russian Academy of Sciences, (IRE RAS), Fryazino, Vvedenskogo sq. 1, 141120 Moscow region, Russia. (agp117@ire216.msk.su)

K. Igarashi and K. Hocke, Communication Research Laboratory, Independent Administrative Institute, 4-2-1, Nukui-Kita Machi, Koganei-shi, Tokyo 184-8795, Japan. (igarashi@crl.go.jp)